Materials
Advances

ROYAL SOCIETY
OF **CHEMISTRY**

PAPER
Sheng Ye, He Li *et al.*
A novel wound dressing based on a gold nanoparticle
self-assembled hydrogel to promote wound healing

ROYAL SOCIETY OF CHEMISTRY

Check for updates

A novel wound dressing based on a gold nanoparticle self-assembled hydrogel to promote wound healing†

Weihong Chen,‡[a] Ruixi Chu,‡[bc] Hualong Li,‡[d] Tianfeng Hua,[a] Hong Chen,[b] Rui Li,[b] Deqing Zhou,[c] Sufeng Cao,[e] Sheng Ye 🆔 *[b] and He Li*[a]

Wound infection and delayed healing not only have a serious impact on human health but also bring a huge economic burden. Therefore, it is particularly important to select an appropriate wound dressing for wound management. Herein, we elaborate the advantages of Au nanoparticles (Au NPs) and a supramolecular hydrogel Nap-Phe-Phe-Tyr (NapFFY) in anti-inflammatory, antibacterial, and wound healing applications, and design and prepare our new wound dressing Au@hydrogel. *In vitro* experiments confirmed that the new dressing had a significant inhibitory effect on the growth of *E. coli* and *S. aureus*, and had great cell biocompatibility, which can be safely used in clinical practice. The *in vivo* experimental results showed that during the 13-day experimental observation period, the combination of Au NPs and the hydrogel could significantly promote wound healing and shorten the wound healing time compared with the use of Au NPs or hydrogel alone. In addition, no obvious toxic or side effects of the dressing on rats were observed during the experiment, and it has great potential for clinical trials in the future. We hope that the combination of Au NPs and supramolecular hydrogels can provide a new strategy for promoting wound healing.

1. Introduction

As the largest organ of the human body, skin plays a vital role in resisting the invasion of exogenous pathogens and regulating temperature, so skin damage will cause serious health problems.[1–3] Once the skin is damaged, our bodies will start the corresponding mechanism to deal with it.[4,5] Generally, wound healing is a complex pathophysiological process involving a variety of biological cascade reactions, which can be generally divided into three stages: inflammatory reaction, new tissue formation, and tissue reconstruction.[6–9] Therefore, effective management must be carried out after skin injury, which is of great significance for accelerating wound healing and maintaining body health.[10] With the continuous progress of modern medical technology, various new materials of dressings are used to promote the rapid healing of wounds. In recent years, hydrogels have been widely used in wound dressing owing to their excellent properties, such as high-water content and similarity to living tissues, and show great potential for development.[11,12] In addition, increasing number of hydrogels are designed as stimulus reaction carriers loaded with drugs or active biomolecules, which can not only protect wounds and reduce infection, but also promote wound healing.[13–15]

Simultaneously, many researchers found that some small molecules have the property of spontaneously assembling into ordered nanofiber structures in water, which can be integrated into gels.[16,17] Many of these gels collectively form a supramolecular gel.[18] In the past 20 years, these gels with supramolecular biological functions have been widely used in wound healing, drug delivery, and functional material design.[19–21] For example, the high-strength and injectable supramolecular hydrogel designed and prepared by Wang's research team has unique therapeutic effects on wound healing after tooth extraction.[22] In addition, the self-assembled DNA THPS hydrogel designed by Rasooly *et al.* has the characteristics of self-healing and injectability.[23] This wound-dressing hydrogel not only has the broad-spectrum antibacterial ability and low cytotoxicity but also can inhibit bacterial diffusion and

[a] *Department of Emergency Surgery & The 2nd Department of Intensive Care Unit, the Second Hospital of Anhui Medical University, Hefei, Anhui 230001, China*

[b] *College of Science & School of Plant Protection, Anhui Agricultural University, Hefei, Anhui 230036, China*

[c] *College of Animal Science and Technology, Anhui Agricultural University, Hefei, Anhui 230036, China*

[d] *People's Hospital of Fengyang County, Chuzhou, Anhui 233100, China*

[e] *Aramco Americas Boston Research Center, 400 Technology Square, Cambridge, MA, 02139, USA*

‡ These authors contributed equally to this work.

accelerate wound healing by releasing THPS, thereby reducing the risk of wound infection. Moreover, its low cost and simple preparation can make it attractive in biomedical applications. In general, supramolecular hydrogels have shown unique advantages in promoting wound healing.[24,25]

In the process of wound healing, bacterial infection is also one of the challenges we must face.[26,27] Severe bacterial infections can aggravate tissue damage, expand inflammatory reactions, and delay the wound-healing process.[28–30] The antibiotics most commonly used to control infection in the past have developed drug resistance due to extensive clinical use, and the treatment effect is far from the previous. Therefore, new materials must be developed to control infection in wound healing. Nanoparticles (NPs) have achieved great success in wound healing and the prevention of wound infection due to their good physical and chemical properties.[31] NPs not only have controllable physical and chemical properties, and can target bacteria at the infection site, but also have a high specific surface area, which can further increase the contact ability with bacteria.[32,33] In addition, the antibacterial properties of NPs can be enhanced by modifying their morphology.[34] Among precious metal NPs used for wound healing, Au NPs are the most commonly used. They have a variety of biological functions, such as antibacterial, anti-inflammatory, and wound healing.[35–39] They are a more rational material used to promote wound healing. At present, there have been many studies on the role of Au NPs in wound healing. For example, the combination of antioxidants and Au NPs designed by Liang et al. can significantly accelerate the healing of diabetic skin wounds through angiogenesis regulation and anti-inflammatory effects and greatly shorten the healing cycle of diabetic ulcer wounds.[40] Meanwhile, another team performed a sun-assisted synthesis of Au NPs based on a hydrogel, which has average size and shape, surface functionalization, antibacterial and wound healing capabilities.[41] In a word, based on the great potential of Au NPs in wound healing, researchers should pay more attention and conduct more in-depth research in the future.

In this work, we are committed to developing efficient wound dressings for wound management. Combining the excellent performance of Au NPs and supramolecular hydrogel Nap-Phe-Phe-Tyr (NapFFY), we designed and prepared a supramolecular hydrogel Au@hydrogel (Scheme 1). Its antibacterial properties were verified through *in vitro* experiments, and its potential in wound healing was studied through *in vivo* experiments, hoping that it can be applied to clinical wound management in the future.

2. Results and discussion

2.1. Preparations of NapFFY, Au@hydrogel, and Au solution

To obtain the supramolecular hydrogel NapFFY gel, 1 mg prepared NapFFY was dissolved in 400 μL TRIS hydrochloride (1 M pH 8.8)/distilled water (volume ratio: 1:1), and then dissolved completely by the ultrasonic dispersion method. The solution was heated up to 90 °C until it became clear. After cooling down to room temperature (25 °C), the transparent NapFFY hydrogel was formed, as shown in Fig. S1 (ESI†). The results of TEM showed that the NapFFY was in the shape of a sea urchin. Further magnification revealed a fibrous appearance. For Au@hydrogel, the same hydrogel precursors were added to the chloroauric acid solution (1 mM) whereafter adding 0.01 M ice-cold $NaBH_4$ sol with ultrasonic processing until the yellowish solution turned wine red. The Nap-Phe-Phe moiety provides the intermolecular π–π stacking and hydrogen bonding, which is the barrier to ensure its self-assembly into hydrogels. Moreover, supramolecular hydrogels formed by self-assembly of small molecules (peptides) through non-covalent interactions are ideal hydrogel forms due to their degradability and biocompatibility, which are much higher than those of polymer hydrogels. The above bath steps were repeated to get the Au@hydrogel (Fig. 1). The addition of Au deepened the color of the sample, and the final sample appeared to resemble an earthworm under transmission electron microscopy. For obtaining a better therapeutic effect, we have a smack at mixing
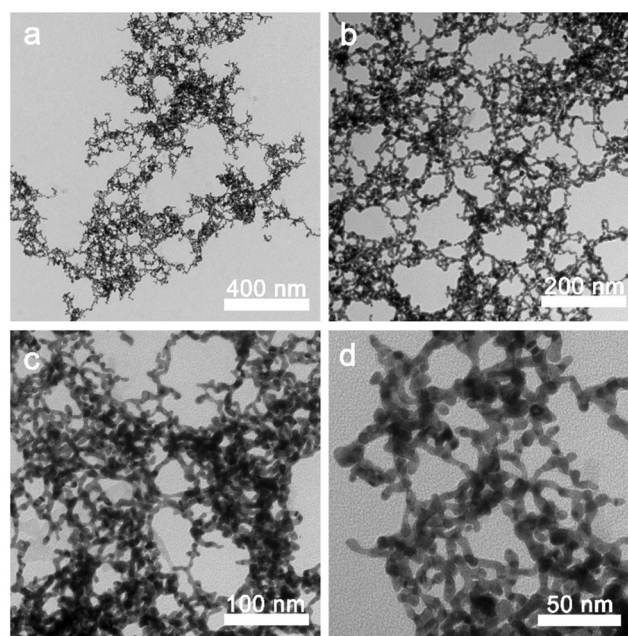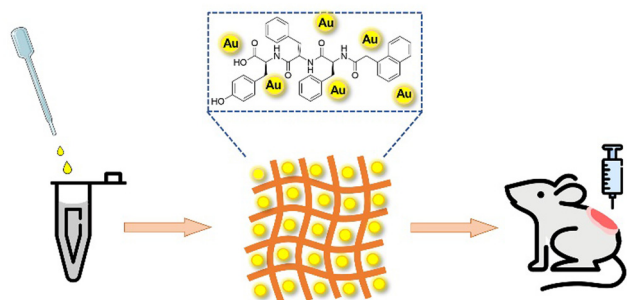

Fig. 1 TEM images at different magnifications of Au@hydrogel, respectively. Image at 20k magnification (a). Image at 40k magnification (b). Image at 80k magnification (c) and image at 150k magnification (d).

Scheme 1 A schematic description of Au@hydrogel for wound healing.

different concentrations of chloroauric acid with hydrogel precursors. Precisely, we tried 25, 50, 75, and 100 μg mL^{-1} chloroauric acid solutions mixed with gel precursors in our pre-experiment, and a mixture of chloroauric acid and gel precursors at 100 μg mL^{-1} was found to have the best effect. About the Au solution, we reached chloroauric acid directly with sodium borohydride solution.

The synthesized supramolecular hydrogel precursors were characterized by nuclear magnetic resonance spectroscopy, and hydrogen spectrum data were obtained (Fig. S2, ESI†) as follows: 1H NMR (600 MHz, DMSO-d$_6$)) δ 8.23 (s, 19H), 7.84 (d, J = 8.4 Hz, 14H), 7.75 (dd, J = 24.7, 8.1 Hz, 19H), 7.57 (s, 12H), 7.49 – 7.43 (m, 15H), 7.35 – 7.09 (m, 84H), 6.99 (d, J = 7.9 Hz, 44H), 6.63 (d, J = 8.1 Hz, 23H), 4.50 (s, 23H), 3.55 (d, J = 14.1 Hz, 16H), 3.52 – 3.22 (m, 274H), 3.29 – 3.22 (m, 13H), 3.29 – 3.22 (m, 13H), 2.91 (ddd, J = 22.6, 20.7, 10.3 Hz, 62H), 2.80 – 2.67 (m, 21H), 2.61 (s, 18H), 2.50 (s, 559H), 2.38 (s, 12H), and −0.00 (s, 53H). Furthermore, the synthesized supramolecular hydrogel precursor was characterized by nuclear magnetic resonance spectroscopy, and the carbon spectrum data obtained (Fig. S3, ESI†) are shown as follows: 13C NMR (151 MHz, DMSO) δ 173.37 (s), 171.44 (s), 170.81 (s), 170.25), 156.13 (s), 138.15 (d, J = 17.8 Hz), 134.23 (s), 133.33 (s), 132.14 (s), 130.62 (s), 129.60 (s), 128.37 (d, J = 20.1 Hz), 127.92 (d, J = 18.5 Hz), 127.77 (dd, J = 20.9, 12.0 Hz), 126.57 (d, J = 16.0 Hz), 126.37 (s), 125.86 (s), 115.30 (s), 54.99 (s), 54.47 (s), 54.21 (s), 42.62 (s), 40.22 (d, J = 20.6 Hz), 40.01 (s), 39.87 (s), 39.73 (s), 39.70 – 39.62 (m), 39.60 (s), 39.52 (d, J = 21.0 Hz), 37.91 (d, J = 9.8 Hz). NMR results all confirmed that the supramolecular hydrogel precursor synthesized in this experiment was NapFFY.

2.2. Biocompatibility performance *in vitro*

After the synthesis of our new dressing, to ensure safer application to animal wound research, we first conducted *in vitro* biocompatibility verification. In the cell compatibility (b) *In vitro* antibacterial activity for *S. aureus*. (c) *In vitro* antibacterial activity for *E. coli.* experiment, we selected L929 cells for co-culture treatment and then detected the activity of the corresponding cells using CCK-8. As shown in Fig. 2a, in the experimental group, the cell activity of cells treated with different concentrations was almost unaffected and even when increasing the concentration of Au NPs to 100 μg mL^{-1}, it remained almost unchanged, demonstrating the non-cytotoxicity of the dressing used. Moreover, to further investigate the blood compatibility of Au@hydrogel, we incubated SD rat red blood cells for 2 hours and removed the supernatant for absorbance detection. As shown in Fig. 2b, almost all red blood cells in the ultrapure water group were ruptured, with a hemolysis rate of 100%. However, when PBS solution and different concentrations of Au@hydrogel were added, red blood cell rupture was relatively rare, and the hemolysis rate was generally below 5%, indicating that Au@hydrogel will not cause damage to red blood cells. Therefore, taking into account the above discussion results, we have chosen an Au NP concentration of 100 μg mL^{-1} combined with the hydrogel for subsequent experimental operation.
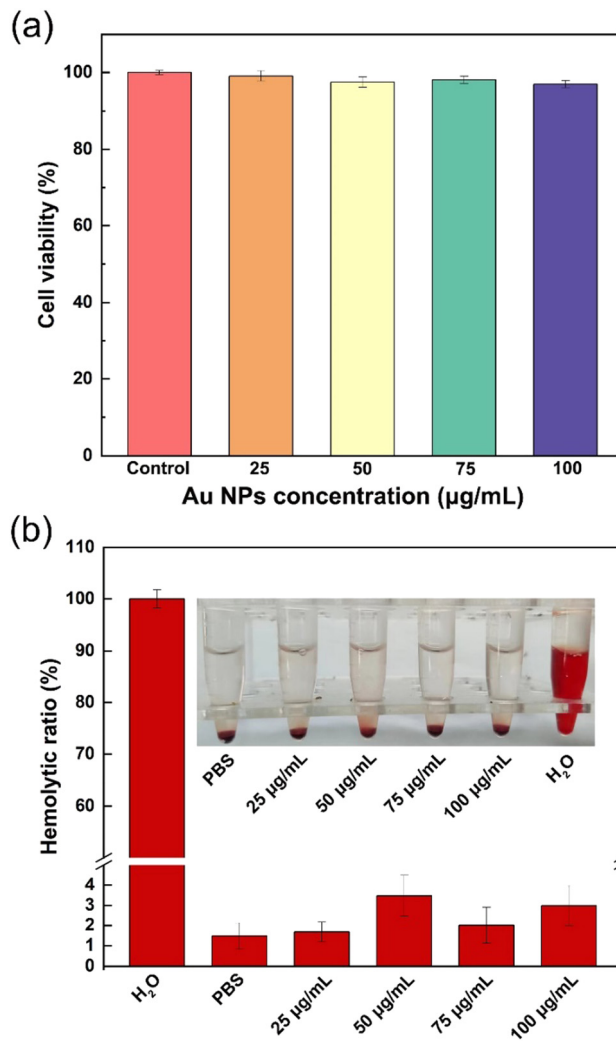

Fig. 2 The safety of Au@hydrogel *in vitro*. (a) Cell viabilities of L929 after being cultured with different concentrations of Au@hydrogel. (b) Hemolysis ratio of red blood cells incubated with Au@hydrogel and the photographs of red blood cells after centrifugation in set.

2.3. Antibacterial performance *in vitro*

The ideal wound dressing should have good antibacterial properties, which are conducive to rapid wound healing. In this study, we selected *S. aureus* (Gram-positive bacterium) and *E. coli* (Gram-negative bacterium) to verify the antibacterial properties of our dressing. As shown in Fig. 3a, in the inhibition experiment on *S. aureus* and *E. coli*, it was found that after 24 hours of culture compared with the control group, the group using Au or hydrogel alone has a significant reduction in bacterial colonies, but the group using our composite dressing Au@hydrogel has the largest reduction in bacterial colonies and the most significant inhibitory effect. In addition, we also made statistics on the sterilization rate of each group (Fig. 3b and c). It was found that the inhibition rate of the group using Au or hydrogel alone on *S. aureus* exceeded half, and the inhibition rate of our composite dressing Au@hydrogel reached 80%. In addition, the inhibition effect on *E. coli* is still
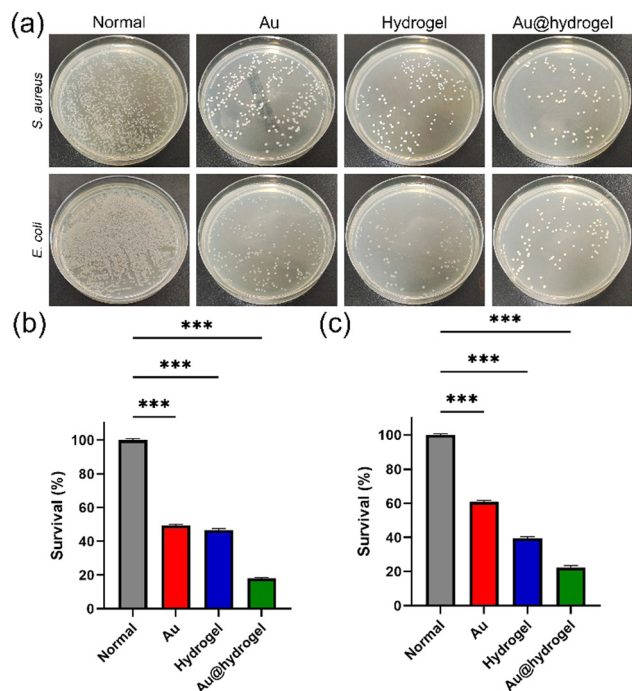
Fig. 3 (a) Photographs of survival bacterial clones of *S. aureus* and *E. coli* on agar plates. (b) *In vitro* antibacterial activity for *S. aureus*. (c) *In vitro* antibacterial activity for *E. coli*.

the best for the compound dressing Au@hydrogel, with an inhibition rate of nearly 80%; however, it is only 40% and 60% for Au and hydrogel used alone. This shows that the composite dressing Au@hydrogel has a significant inhibitory effect on the growth of bacteria, and its effect is due to the use of Au or hydrogel alone, showing its great potential in antibacterial applications.

2.4. Weight changes in rats

24 SD rats (male, 3–4 months old, weighing 240 ± 10 g) were obtained from the experimental center. They had been fed adaptively for one week before being randomly divided into 4 groups for the experiment. The rats were in good condition during feeding. As shown in Fig. 4, we can see that on the first day, after the establishment of the wound model, the weight of rats in each group decreased slightly, which may be caused by the anesthesia and acute traumatic stress during the experiment, which made them unable to return to normal diet in time. After the first day of adaptation, the weight of rats increased steadily in the follow-up experimental observation process, and there was no significant difference in weight changes between groups. It can be seen that the impact of acute trauma on rats is gradually eliminated, and the establishment of a wound model has not caused a serious impact on rats.

2.5. Incision wound experiment

To verify the healing of the incision wound with our material, we successfully created an incision wound in rats. As shown in
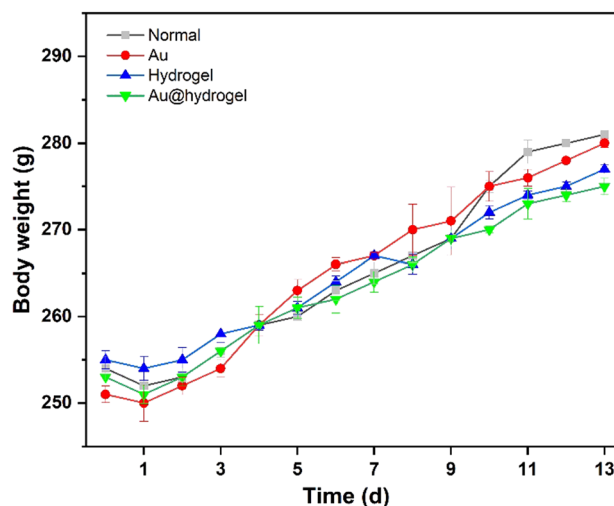

Fig. 4 The body weight of SD rats was recorded throughout the experiment.

Fig. S4 (ESI†), we noticed that on the third day of experimental observation, the healing of the hydrogel group and the Au@hydrogel group was similar, both of them had partial scabbing, and the scope was smaller than before. On the 7th day, there was a certain difference between the two groups. The Au@hydrogel group had better healing, and the wound area was significantly reduced. On the 12th day, it can be seen that the scabs in the Au@hydrogel group have fallen off completely, and a small part of the scabs remains in the hydrogel group, but the wounds of the two groups have healed. The curative effect of using hydrogel alone is not as good as that of Au@hydrogel.

2.6. Wound closure evaluation of full-thickness skin incision

We established a full-thickness skin incision model to verify that Au@hydrogel has great potential in promoting wound healing (Scheme 2). After the rat model was established successfully, the wound healing was observed daily. As shown in Fig. 5, on the third day of the experiment, the wounds of each group were shrunk to varying degrees compared with the initial. In the normal group without any treatment, a large number of blood scabs were formed, the infection around the wound was severe, and the degree of healing was minimal. The healing of the hydrogel and Au treated groups was similar, and the blood scab around the wound was small. The rats treated with Au@hydrogel showed the best healing among the four groups. Not only was the wound area significantly smaller, and blood scabs were rarely seen, but also no obvious infection was observed. It shows that Au@hydrogel treatment can effectively
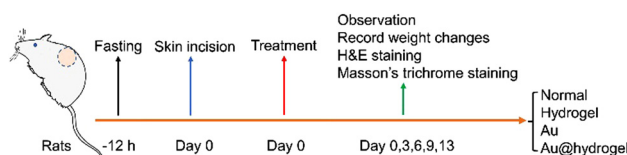
Scheme 2 Schematic diagram of skin incision modeling and treatment process.
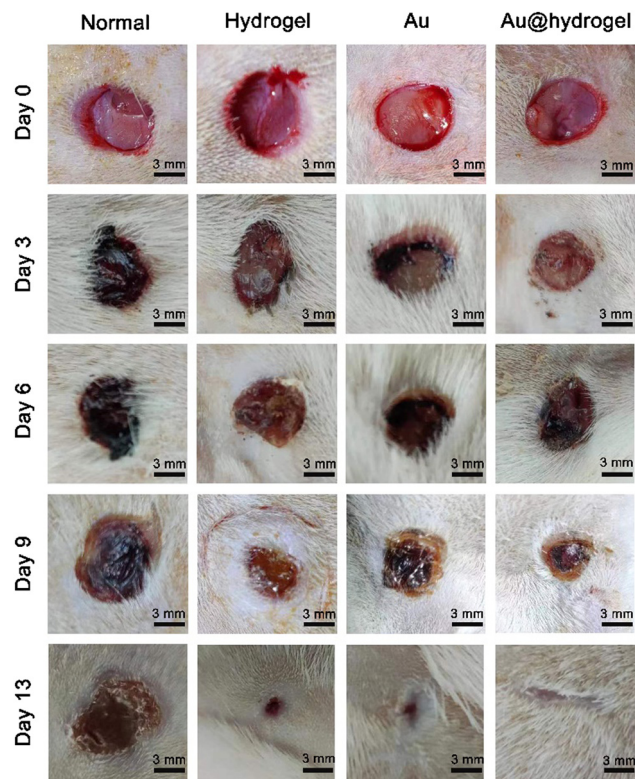
Fig. 5 Rats were submitted to skin excision on day 0. Representative macroscopic images of the wound closure on postoperative days 3, 6, 9, and 13 in normal, hydrogel, Au, and Au@hydrogel groups.

promote wound healing. On the 6th day of treatment, the wounds of each group were scabbed to varying degrees, and the range was also narrowed compared with the progress. The Au@hydrogel group still had the best healing. By the 9th day of treatment, the scab of large pieces in the Au@hydrogel group had fallen off, and the wound scope was significantly reduced. However, the untreated control group still had a large number of scabs at this time, and the wound scope was not significantly reduced compared with that before. On the 13th day of treatment, the wound treated with Au@hydrogel has basically healed, the hair around it grows vigorously, and the wound can hardly be seen on the surface. The untreated control group still had a lot of scabs left at this time, and the wound area was still large, which showed that the healing was not good. In the case of Au and hydrogel treatment alone, a small area of the wound still exists, but the scab on it has fallen off, and the healing is less than that of Au@hydrogel treatment. What's more, as shown in Fig. 6, we measured the wound area to more accurately reflect the healing of each group. After 13 days of healing, the wound healing speed of the Au@hydrogel group was very fast, which was close to the normal skin at this time. The healing speed of the group using Au or hydrogel alone was slower, while the wound healing speed of the normal control group at this time was the slowest among the four groups. In general, the wound dressing we used has a good healing effect, can significantly shorten the time required for wound healing, and shows its great potential to promote wound healing.
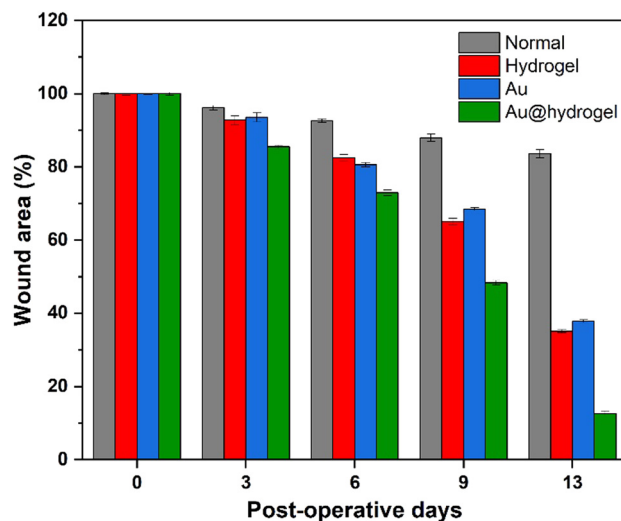

Fig. 6 The average wound area percentage in the experimental days of different groups, with postoperative day 0 considered 100%.

2.7. Histomorphological evaluation of wound regeneration

The inflammation reaction stage, tissue regeneration stage, and tissue reconstruction stage are three closely related necessary stages in the wound healing process.[42,43] On the 3rd, 6th, 9th, and 13th days of the experiment, the wound tissues were obtained, respectively, and the histological morphology of wound regeneration at different stages was determined by H&E staining and Masson staining. As shown in Fig. 7, on the third day, the wounds in each group were in the acute inflammatory stage, and a large number of inflammatory cells, such as neutrophils, were seen infiltrating, and epithelial tissue was absent. At this time, the wound did not show an obvious proliferation of fibers and skin appendages such as hair follicles, but a small number of new capillaries were still observed in the Au@hydrogel treatment group, indicating that the wound had entered the tissue proliferation stage at this
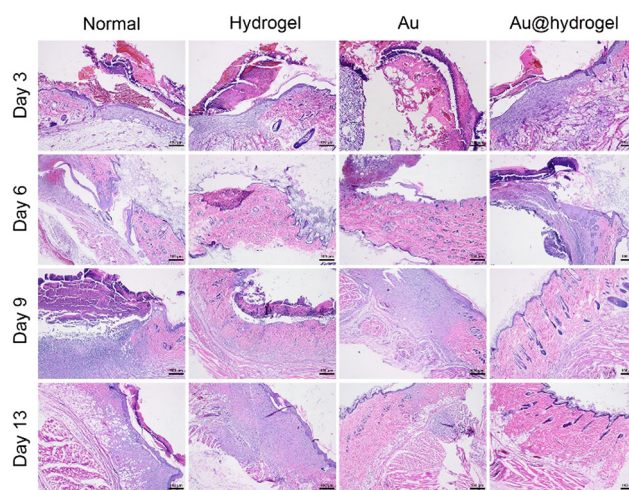

Fig. 7 Representative H&E staining images of skin incisions after healing for 3, 6, 9, and 13 days (scale bar = 100 μm).
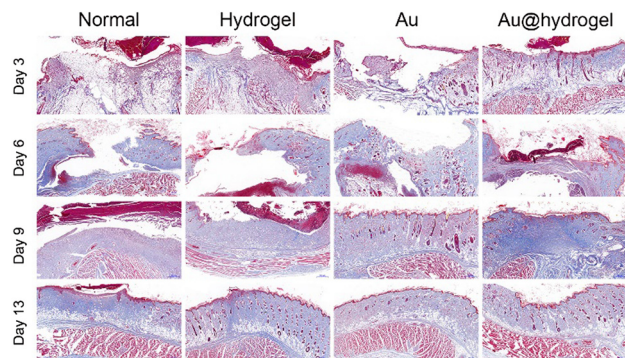
Fig. 8 Representative images of Masson trichrome staining of skin incision after 3, 6, 9, and 13 days of healing (scale bar = 500 μm).

time, and the wound healing speed was significantly faster than that of other groups. After several days of continuous healing, the tissue section on the 6th and 9th days still the healing of the Au@hydrogel treatment group better than that of other groups. On the 13th day, the wound tissue treated with Au@hydrogel was the same as the normal tissue, with abundant new blood vessels and a large number of hair follicles. The untreated control group had improved inflammation at this time, but there was still less new tissue, indicating that the healing was general. The healing of the other two groups was similar, but still inferior to that of the Au@hydrogel group. Not only that, but we also performed Masson staining on the obtained wound tissue to further evaluate wound regeneration. As shown in Fig. 8, on the third day of the experiment, the existence of some blue-stained collagen fibers can be observed in the Au@hydrogel group, and the number of red-stained muscle fibers is still small, indicating the initial stage of tissue proliferation at this time; the number of collagen fibers in other groups is less at this time and the number of muscle fibers in the control group is the largest, indicating that the control group has not entered the tissue proliferation period at this time. After a few days of healing, on the 13th day, a small amount of blue-stained collagen fibers was observed in the untreated control group, while the number of collagen fibers in the tissues treated with Au and hydrogel alone was significantly higher than that in the control group. At this time, the blue-stained collagen fibers in the tissues treated with Au@hydrogel were the most in the four groups. In addition, a large number of new capillaries and hair follicles were also observed in the slices of this group, this shows that the healing of this group is the best, and the histomorphological evaluation fully reflects that the product Au@hydrogel, which is a combination of Au and hydrogel, has great potential in promoting wound healing.

3. Experimental

3.1. Materials

The materials used were as follows: $NaBH_4$, $HAuCl_4 \cdot 4H_2O$, Tris–HCl (1 M, pH 8.8), 2-naphthylacetic acid (abbreviated to Nap), Fmoc-Tyr (tBu)-OH ($C_{28}H_{29}NO_5$, abbreviated to Y), Fmoc-Phe-OH

($C_{24}H_{21}NO_4$, abbreviated to F), 2-chlorotrityl chloride resin, methanol (CH_3OH), dichloromethane (methylene chloride, abbreviated to DCM, CH_2Cl_2), trifluoroacetic acid (abbreviated to TFA, CF_3COOH). The main experimental materials were purchased from biosharp, Shanghai-yuanyeBio-Technology Co., Ltd, Shanghai McLean Biochemical Technology Co., Ltd, Shanghai RichJoint Chemical Reagents Co., Ltd, Chengdu Xilong Chemical Reagent Glassware Co., Ltd, and Shanghai Hushi Chemical Co., Ltd. All the agencies were selected superior purity or higher, all of which held their original purity unless we have special instructions.

3.2. Synthesis of Au@hydrogel

Based on the existing work base of our laboratory, under the method of solid-state synthesis, Fmoc-Tyr (tBu)-OH was connected to 2-trichloroyl chloride resin with multiple active sites by dehydration condensation.[18] Then, the unreacted active sites on the resin were sealed with methanol, and two fmoc-fe-OH and 2-naphthoacetic acid were connected to obtain NapFFY resin. Additionally, 300 mL DCM containing 1% TFA was added to separate NapFFY from the resin. The collected liquid was purified and freeze-dried to obtain a supramolecular hydrogel precursor (NapFFY). The supramolecular hydrogel precursor powder (NapFFY) is a white solid powder, consisting of self-assembly to form small molecules (peptides) through non-covalent interactions, and is more biocompatible and degradable than polymer hydrogels. Then an appropriate amount of NapFFY was added into Tris–HCl solution until dissolved completely, while adding the cold $NaBH_4$ solution and $HAuCl_4$ solution at the same time. Dissolution was performed, and the mixture was sonicated in a 90 °C-water bath for a moment. Within a few minutes, the temperature had cooled, and the previous liquid had thickened enough to become a gelatinous precipitate (Au@hydrogel).

3.3. *In vitro* biocompatibility

To verify the biocompatibility of the new dressing, we selected mouse fibroblasts (L929) for *in vitro* experiments. Firstly, different concentrations of Au@hydrogel were placed on a 96-well culture plate, and the recovered L929 cells were seeded on the plate and incubated overnight at 37 °C. After 48 hours, we replaced the old cell culture medium with a fresh RMPI1640 containing CCK-8 test solution. After incubation for 2 hours, absorbance was measured to calculate the cell activity of each group. In addition, we conducted *in vitro* hemolysis experiments using SD rat red blood cells to evaluate the hemolysis rate of Au@hydrogel. Firstly, whole blood was obtained from healthy SD rats using the eyeball blood collection method, collected in an anticoagulant tube, shaken evenly, and centrifuged at 3000 rpm for 10 minutes to obtain red blood cells. Different concentrations of Au NPs were prepared, and 1 mL of different concentrations of Au@hydrogel, 1 mL of PBS solution, and 1 mL of ultrapure water were placed in an EP tube. 20 microliters of red blood cells were added and incubated for 2 hours. Finally, the hemolysis rate was calculated by

measuring the absorbance value of the supernatant after centrifugation.

3.4. *In vitro* antibacterial activity

To verify the antibacterial properties of our synthetic dressing, *E. coli* (ATCC 25922) and *S. aureus* (ATCC 29213) were selected for the experiment. 100 μL hydrogel was successfully prepared and spread in a 48-well culture plate. After the temperature was cooled to glue, 20 μL sterile PBS solution dissolved in bacterial suspension (10^6 CFU mL^{-1}) was injected into the 48-well culture plate, and slightly shaken to make it evenly distributed. The inoculated culture plate was incubated at 37 °C for 2 hours, and the internal humidity of the culture plate was kept unchanged. After the time was over, 1 mL of sterile PBS solution was added to each well to suspend viable cells. Finally, 20 μL of the bacterial suspension obtained from each group was inoculated on the agar plate, and incubated in the incubator at 37 °C for 24 hours, and photos were taken and the colonies on the plate were counted after they formed.

3.5. Incision wound experiment

Male SD rats weighing 240 ± 10 g and aged 3–4 months were obtained from the experimental center. All rats were fed adaptively for one week before the experiment. Before the experiment, all rats were randomly divided into 2 groups: the hydrogel group and the Au@hydrogel group. The routine anesthesia procedure was carried out, and pentobarbital (50 mg kg^{-1}) was injected intraperitoneally to ensure that all rats were under anesthesia and that the vital signs measured were normal. We used scissors to cut off the long hair in the perforated area in advance, applied hair removal cream for hair loss, and then completely cut off the remaining hair in the surgical area. Then, the remaining depilatory cream was rinsed with pure water. After full disinfection with 75% alcohol, the sterile surgical blade was used to cut a wound with a length of 1 cm on the back of the rat, without injuring the fascia and muscle. In this way, we successfully established an incision wound model.

3.6. *In vivo* wound healing of a full-thickness skin defect model

Our animal experiments have been approved by the Animal Experiment Ethics Committee. Male SD rats weighing 240 ± 10 g and aged 3–4 months were obtained from the experimental center. All rats were randomly divided into 4 groups before the experiment, including the normal group, Au group, hydrogel group, and Au@hydrogel group. All rats were fed adaptively for one week before the experiment. After an intraperitoneal injection of pentobarbital (50 mg kg^{-1}), it was confirmed that all rats were under anesthesia and maintained normal respiration and heartbeat, with no obvious abnormality in vital signs. We used scissors to cut off the long hair on the perforated part in advance, applied depilatory cream, and after taking effect, completely removed the hair on the operation area of rats. The back of the rats was thoroughly disinfected and the standard perforator was used to establish a round symmetrical wound with a diameter of 8 mm on the back of the rats. After the wound model was established successfully, the experiment was conducted according to the groups. On the 3rd and 13th days, the skin tissues of 6 rats in each group of 4 groups were collected. The wound regeneration process was evaluated by wound area and histomorphology. For wound area monitoring, digital cameras were used to record the wound healing process after anesthesia at a specific time every day on the 3rd, 6th, 9th, and 13th days. All samples were stored at −80 °C before the histological examination.

3.7. Histomorphological determination

To evaluate the tissue regeneration and inflammation in the wound area, wound samples of each group were collected on the 3rd and 13th days. The collected skin samples were first fixed with 4% paraformaldehyde for 1 hour and then embedded in paraffin for preservation. Next, we cut the paraffin-embedded skin tissue into thin slices with a thickness of 4 μm. The sagittal sections were stained with hematoxylin and eosin (H&E), and Masson in three colors to observe the regeneration of wound tissues and skin appendages, and photographs were taken with a microscope.

Conclusions

In summary, Combining the advantages of Au NPs and NapFFY supramolecular hydrogel in promoting wound healing, we designed and prepared a new supramolecular hydrogel wound dressing Au@hydrogel. *In vitro* experiments confirmed that it has excellent antibacterial properties and can reduce bacterial infection during wound healing. It also has excellent cell biocompatibility and can be safely used for *in vivo* experiments. *In vivo* experiments have proved that the dressing can be safely used for wounds with less toxicity and side effects. In addition, it can significantly shorten the time of wound healing and has great potential for clinical wound healing management. We believe that the supramolecular hydrogel Au@hydrogel can be used clinically to promote wound healing in the near future.

Author contributions

Weihong Chen: conceptualization, data curation, investigation, methodology, writing – original draft; Ruixi Chu: data curation, investigation, methodology, writing – original draft; Hualong Li: data curation, investigation, methodology, writing – original draft; Tianfeng Hua: data curation, investigation; Hong Chen: data curation; Rui Li: methodology; Deqing Zhou: data curation; Sufeng Cao: conceptualization; Sheng Ye: funding acquisition, supervision; He Li: funding, acquisition, supervision.

Conflicts of interest

The authors declare no conflict of interest.

Acknowledgements

References

1 M. K. Strecker-McGraw, T. R. Jones and D. G. Baer, *Emerg. Med. Clin. N. Am.*, 2007, **25**, 1.

2 C. K. Sen, G. M. Gordillo, S. Roy, R. Kirsner, L. Lambert, T. K. Hunt, F. Gottrup, G. C. Gurtner and M. T. Longaker, *Wound Repair Regen.*, 2009, **17**, 763.

3 G. C. Gurtner, S. Werner, Y. Barrandon and M. T. Longaker, *Nature*, 2008, **453**, 314.

4 H. N. Wilkinson and M. J. Hardman, *Open Biol.*, 2020, **10**, 200223.

5 E. A. Gantwerker and D. B. Hom, *Facial Plast. Surg. Clin.*, 2011, **19**, 441.

6 P. Bao, A. Kodra, M. Tomic-Canic, M. S. Golinko, H. P. Ehrlich and H. Brem, *J. Surg. Res.*, 2009, **153**, 347.

7 T. J. Shaw and P. Martin, *J. Cell Sci.*, 2009, **122**, 3209.

8 P. H. Wang, B. S. Huang, H. C. Horng, C. C. Yeh and Y. J. Chen, *J. Chin. Med. Assoc.*, 2018, **81**, 94.

9 A. Hassanshahi, M. Hassanshahi, S. Khabbazi, Z. Hosseini-Khah, Y. Peymanfar, S. Ghalamkari, Y. W. Su and C. J. Xian, *J. Cell. Physiol.*, 2019, **234**, 7903.

10 A. Maleki, J. He, S. Bochani, V. Nosrati, M. A. Shahbazi and B. Guo, *ACS Nano*, 2021, **15**, 18895.

11 J. S. Boateng, K. H. Matthews, H. N. Stevens and G. M. Eccleston, *J. Pharm. Sci.*, 2008, **97**, 2892.

12 J. Koehler, F. P. Brandl and A. M. Goepferich, *Eur. Polym. J.*, 2018, **100**, 1.

13 N. Sood, A. Bhardwaj, S. Mehta and A. Mehta, *Drug Delivery*, 2016, **23**, 758.

14 O. Guaresti, C. García-Astrain, R. H. Aguirresarobe, A. Eceiza and N. Gabilondo, *Carbohydr. Polym.*, 2018, **183**, 278.

15 Y. Liang, Z. Li, Y. Huang, R. Yu and B. Guo, *ACS Nano*, 2021, **15**, 7078.

16 M. C. Cringoli, S. Marchesan, M. Melchionna and P. Fornasiero, *Molecules*, 2020, **25**, 5620.

17 N. M. Sangeetha and U. Maitra, *Chem. Soc. Rev.*, 2005, **34**, 821.

18 J. Zhu, R. Hou, M. Liu, L. Wang, W. Chen, Y. Sun, W. Wei and S. Ye, *Mater. Today Sustainability*, 2022, **18**, 100125.

19 M. S. Hu, Z. N. Maan, J. C. Wu, R. C. Rennert, W. X. Hong, T. S. Lai, A. T. Cheung, G. G. Walmsley, M. T. Chung, A. McArdle, M. T. Longaker and H. P. Lorenz, *Ann. Biomed. Eng.*, 2014, **42**, 1494.

20 N. L. Delgadillo-Armendariz, N. A. Rangel-Vázquez and A. I. García-Castañón, *Spectrochim. Acta, Part A*, 2014, **120**, 524.

21 Y. Liang, J. He and B. Guo, *ACS Nano*, 2021, **15**, 12687.

22 Z. Wang, Y. Zhang, Y. Yin, J. Liu, P. Li, Y. Zhao, D. Bai, H. Zhao, X. Han and Q. Chen, *Adv. Mater.*, 2022, **34**, 2108300.

23 X. Jiang, M. Li, X. Guo, M. Yang and A. Rasooly, *ACS Appl. Bio. Mater.*, 2019, **2**, 1262.

24 J. Omar, D. Ponsford, C. A. Dreiss, T. C. Lee and X. J. Loh, *Chem. – Asian J.*, 2022, **17**, 202200081.

25 Y. Zhang, Y. Kuang, Y. Gao and B. Xu, *Langmuir*, 2011, **27**, 529.

26 M. A. Mofazzal Jahromi, P. Sahandi Zangabad, S. M. Moosavi Basri, K. Sahandi Zangabad, A. Ghamarypour, A. R. Aref, M. Karimi and M. R. Hamblin, *Adv. Drug Deliverery Rev.*, 2018, **123**, 33.

27 Y. Wang, J. Beekman, J. Hew, S. Jackson, A. C. Issler-Fisher, R. Parungao, S. S. Lajevardi, Z. Li and P. K. M. Maitz, *Adv. Drug Deliverery Rev.*, 2018, **123**, 3.

28 R. Edwards and K. G. Harding, *Curr. Opin. Infect. Dis.*, 2004, **17**, 91.

29 P. G. Bowler, *Ann. Med.*, 2002, **34**, 419.

30 Y. Huang, L. Mu, X. Zhao, Y. Han and B. Guo, *ACS Nano*, 2022, **16**, 13022.

31 A. Naskar and K. S. Kim, *Pharmaceutics*, 2020, **12**, 499.

32 M. Liu, J. Zhu, Y. Liu, F. Gong, R. Li, H. Chen, M. Zhao, Q. Jiang, J. Liu and S. Ye, *Chem. Eng. J.*, 2022, **446**, 137080.

33 J. Zhu, W. Chen, Y. Sun, X. Huang, R. Chu, R. Wang, D. Zhou and S. Ye, *Mater. Adv.*, 2022, **3**, 7687.

34 R. Y. Pelgrift and A. J. Friedman, *Adv. Drug Delivery Rev.*, 2013, **65**, 1803.

35 S. C. Wei, L. Chang, C. C. Huang and H. T. Chang, *Biomater. Sci.*, 2019, **7**, 4482.

36 W. E. Soliman, H. S. Elsewedy, N. S. Younis, P. Shinu, L. E. Elsawy and H. A. Ramadan, *Polymers*, 2022, **14**, 2637.

37 Q. Zhang, M. Li, B. Luo, Y. Luo, H. Jiang, C. Chen, S. Wang and D. Min, *J. Hazard. Mater.*, 2021, **402**, 123445.

38 A. U. Khan, Q. Yuan, Y. Wei, G. M. Khan, Z. U. H. Khan, S. Khan, F. Ali, K. Tahir, A. Ahmad and F. U. Khan, *J. Photoch. Photobio. B*, 2016, **162**, 273.

39 S. J. Hwang, S. H. Jun, Y. Park, S. H. Cha, M. Yoon, S. Cho, H. J. Lee and Y. Park, *Nanomedicine*, 2015, **11**, 1677.

40 S. A. Chen, H. M. Chen, Y. D. Yao, C. F. Hung, C. S. Tu and Y. J. Liang, *Eur. J. Pharm. Sci.*, 2012, **47**, 875.

41 Z. Batool, G. Muhammad, M. M. Iqbal, M. S. Aslam, M. A. Raza, N. Sajjad, M. Abdullah, N. Akhtar, A. Syed, A. M. Elgorban, S. S. Al-Rejaie and Z. Shafiq, *Sci. Rep.*, 2022, **12**, 6575.

42 M. Takeo, W. Lee and M. Ito, *CSH Perspect. Med.*, 2015, **5**, 023267.

43 S. Guo and L. A. Dipietro, *J. Dent. Res.*, 2010, **89**, 219.